

Quantum phase transitions in the spin-boson model without the counterrotating terms

Yan-Zhi Wang¹, Shu He², Liwei Duan¹, and Qing-Hu Chen^{1,3,*}

¹ *Department of Physics, Zhejiang University, Hangzhou 310027, P. R. China*

² *Department of Physics and Electronic Engineering, Sichuan Normal University, Chengdu 610066, China*

³ *Collaborative Innovation Center of Advanced Microstructures, Nanjing University, Nanjing 210093, China*

(Dated: December 11, 2018)

We study the spin-boson model without the counterrotating terms by a numerically exact method based on variational matrix product states. Surprisingly, the second-order quantum phase transition (QPT) is observed for the sub-Ohmic bath in the rotating-wave approximations. Moreover, the mean-field criticality is demonstrated for all bath exponents $0 < s < 1$, in contrast to the full spin-boson model. For large value of the bath exponent, a few first-order QPTs also appear before the critical points. With the decrease of the bath exponents, these first-order QPTs disappear successively, while the second-order QPT remains robust. The second-order QPT is further confirmed by multi-coherent-states variational studies, while the first-order QPT is corroborated with the exact diagonalization in the truncated Hilbert space. Extension to the Ohmic bath is also performed, and many first-order QPTs appear successively in a wide coupling regime. The previous picture for many physical phenomena based on the conserved total excitations in open quantum systems might be not valid at least for sub-ohmic baths at the strong coupling.

PACS numbers: 03.65.Yz, 03.65.Ud, 71.27.+a, 71.38.k

I. INTRODUCTION

Spin-boson model describes a qubit (two-level system) coupled to a quantum environment represented by a continuous bath of bosonic modes. It is a paradigmatic model in many fields, ranging from quantum optics [2], condensed matter physics [1], to open quantum systems [3, 4]. In most theoretical studies, the rotating-wave approximation (RWA) is usually employed mainly due to the weak coupling strength in the real quantum optical and quantum dissipative systems. In the RWA, the total excitations should be conserved due to the $U(1)$ symmetry, which can considerably simplify the problems and discussions. In this way, the counter-rotating contributions involved higher excited states are neglected. It is generally believed that RWA is a reasonably good approximation because the counter-rotating terms violate energy conservation, leading to virtual processes, and thus are suppressed.

With the advance of technology, the various qubit and oscillator coupling systems can be engineered in many solid-state devices, such as superconducting circuits [5, 6], cold atoms [7], and trapped-ions [8]. Recently, the spin-boson model has been realized by the ultrastrong coupling of a superconducting flux qubit coupled to an open 1D transmission line [9]. The counterrotating terms can be strongly suppressed in some proposed schemes [10–12]. In some systems, the anisotropy appears quite naturally, because they are controlled by different input parameters [13]. On the theoretical side, the anisotropic models, where the rotating and counterrotating terms are different, have attracted considerable attentions. The rich phase diagram in the anisotropic Dicke model including the Tavis-Cummings model [14] where counter-rotating terms are not included has been reported [11]

in the thermodynamic limit, i.e. infinite qubits. It is found in [15] that Jaynes-Cummings (JC) model [16], the quantum Rabi model in the RWA, could undergo the second-order quantum phase transition (QPT) in the extreme model parameter limit, $\Delta/\omega \rightarrow \infty$ where Δ and ω are the frequencies of qubit and cavity. It was demonstrated that the ratio of frequencies Δ/ω plays the same role of the qubits number N . The second-order QPT can be identified by the finite frequency scaling analysis.

Since both the Dicke and Rabi models in the RWA undergo the second-order QPT, then whether the spin-boson model in the RWA can display the second-order QPT? Are some extreme conditions for model parameters required to realize the second-order QPT? As we know that in the literature and textbooks, the spin-boson Hamiltonian with the RWA is usually treated in the sub-space with the fixed total excitations. In this way the second-order QPT is absolutely excluded. The constrained condition for the given sub-space should be relaxed to detect more physical phenomena.

In the spin-boson model without the RWA, the second-order QPT from delocalized phase to localized phase only emerges in the sub-Ohmic bath. Many advanced numerical approaches in the quantum many-particle physics have been applied and extended to this model, such as the numerical renormalization group [17], quantum Monte Carlo simulations [18], sparse polynomial space approach [19], exact diagonalization in terms of shift bosons [20], and various matrix product state approaches [21, 22]. Some analytical approaches based on the polaronic unitary transformation also known as Silbey-Harris ansatz [23] have been also developed for this model [24–32]. The single coherent states ansatz [23] was improved by simply adding other coherent states on the equal footing [28] and by superpositions of two degenerate single coherent states [27], which are generally termed as multi-

coherent-states (MCS) ansatz. Actually, the MCS in the single-mode model has been proposed much earlier by Ren *et al.* [33].

In this work, we will extend the variational matrix product state (VMPS) approach [21] to study the spin-boson model in the RWA for all values of the bath exponents. The MCS variational approach and exact diagonalization within truncated Hilbert space are also employed to provide independent check in different regimes. The paper is organized as follows: In section II, we briefly introduce the spin-boson model in the RWA. Some methodologies including the VMPS, the MCS variational approaches, and exact diagonalization in truncated Hilbert space are described. The rich phase transitions revealed by the VMPS method are presented in section III, where the MCS variational approaches and the exact diagonalization are also applied to provide further evidence. The quantum criticality based on VMPS studies is also analyzed. Finally, conclusions are drawn in section IV.

II. MODEL HAMILTONIAN AND METHODOLOGIES

The anisotropic spin-boson Hamiltonian can be written as ($\hbar = 1$)

$$\begin{aligned} \hat{H}_{SB} = & \frac{\Delta}{2}\sigma_z + \sum_k \omega_k a_k^\dagger a_k + \frac{1+\lambda}{2} \sum_k g_k (a_k^\dagger \sigma_- + a_k \sigma_+) \\ & + \frac{1-\lambda}{2} \sum_k g_k (a_k \sigma_- + a_k^\dagger \sigma_+), \end{aligned} \quad (1)$$

where $\sigma_\pm = (\sigma_x \pm i\sigma_y)/2$ with σ_i ($i = x, y, z$) the Pauli matrices, Δ is the tunneling amplitude between the spin-up state $|\uparrow\rangle$ and the spin-down state $|\downarrow\rangle$, a_k (a_k^\dagger) is the bosonic annihilation (creation) operator which can annihilate(create) a boson with frequency ω_k . $\frac{1+\lambda}{2}$ and $\frac{1-\lambda}{2}$ are the weights of the rotating-wave and counter rotating-wave terms respectively. In this sense λ is the anisotropy constant of this model. Obviously, $\lambda = 1$ ($\lambda = 0$) correspond to the spin-boson model with (without) RWA. g_k denotes the coupling strength between the qubit and the bosonic bath, which is characterized by the spectral density $J(\omega)$,

$$J(\omega) = \pi \sum_k g_k^2 \delta(\omega - \omega_k) = 2\pi\alpha\omega_c^{1-s}\omega^s \Theta(\omega_c - \omega), \quad (2)$$

where α is a dimensionless coupling constant, ω_c is the cutoff frequency, and $\Theta(\omega_c - \omega)$ is the Heaviside step function. The bath exponent s classifies the reservoir into super-Ohmic ($s > 1$), Ohmic ($s = 1$), and sub-Ohmic ($s < 1$) types respectively.

For later use, Hamiltonian (1) can be rewritten as

$$\begin{aligned} \hat{H} = & \frac{\Delta}{2}\sigma_z + \sum_k \omega_k a_k^\dagger a_k + \frac{1}{2} \sum_k g_k (a_k^\dagger + a_k) \sigma_x \\ & + \frac{\lambda}{2} \sum_k g_k (a_k - a_k^\dagger) i\sigma_y. \end{aligned} \quad (3)$$

In the following, we introduce three methods.

VMPS approach.- As is well known, VMPS approach works efficiently in one-dimensional chain models [34, 35]. To apply VMPS in the spin-boson model, we therefore transform the model into a 1D chain model. We first perform the logarithmic discretization of the spectral density of the continuum bath [17] with discretization parameter $\Lambda > 1$, then by using orthogonal polynomials $b_n^+ = \sum_k U_{nk} a_k^+$ ($b_n = \sum_k U_{nk} a_k$) as described in Ref. [36], the spin-boson models can be mapped into the representation of an one-dimensional semi-infinite chain with nearest-neighbor interaction (see details in Ref. [37]). Thus, Hamiltonian (3) can be written as:

$$\begin{aligned} H_{\text{chain}} = & \frac{1}{2}\Delta\sigma_z + \frac{c_0}{2}(b_0 + b_0^\dagger)\sigma_x + \lambda\frac{c_0}{2}(b_0 - b_0^\dagger)i\sigma_y \\ & + \sum_{n=0}^{L-2} [\epsilon_n b_n^\dagger b_n + t_n (b_n^\dagger b_{n+1} + b_{n+1}^\dagger b_n)], \end{aligned} \quad (4)$$

where b_n^\dagger (b_n) is creation(annihilation) operator for a new set of boson modes in transformed representation with ϵ_n describing frequency on chain site n , t_n describing the nearest-neighbor hopping parameter, and c_0 describing the effective coupling strength between the spin and the new effective bath. All of parameters mentioned above, such as t_n , ϵ_n and c_0 , are determined by the logarithmic discretization parameter Λ , the cutoff frequency ω_c and the specific form of the spectral density.

Then we briefly introduce the VMPS approach [38–40]. For the transformed spin-boson model of 1D chain with L sites, the ground state wave function of Hamiltonian (4) can be depicted as

$$|\psi\rangle = \sum_{\{N_n\}=1}^{d_n} M[N_1] \dots M[N_L] |N_1, \dots, N_L\rangle, \quad (5)$$

where N_n is the physical dimension of each site n with truncation d_n , and D_n is the bond dimension for matrix M with the open boundary condition, bounding the maximal entanglement in each subspace. M on each site is optimized through sweeping the 1D chain iteratively, where accuracy of numerical results is determined by values of d_n and D_n . In order to deal with spin-boson model near the quantum critical region effectively, we apply an optimized boson basis through an additional isometric map with $d_{\text{opt}} \ll d_n$ like in Refs. [21, 37]. In this way, we can effectively reduce local boson basis and improve the maximum of boson number in quantum critical region.

In this paper, we mainly focus on phase transitions of the RWA model with sub-ohmic spectral density, namely

$\lambda = 1$, $0 < s < 1$. For the data presented below, we typically choose the model parameters as $\Delta = 0.1$, $\omega_c = 1$. Some parameters of orthogonal polynomials transformation and VMPS are the same as those in Ref. [21], e.g. the logarithmic discretization parameter $\Lambda = 2$, the length of semi-infinite chain $L = 50$, optimized truncation numbers $d_{opt} = 12$. In addition, we adjust the bond dimension to achieve better convergence of the results. In this work, we choose $D_{max} = 20, 60$ for $s = 0.3, 0.7$ respectively, which is sufficient to obtain the converging results.

Exact diagonalization in truncated Hilbert space.- Note also that the spin-boson model with the RWA possesses the $U(1)$ symmetry, the total excitation number $\hat{N} = \sum_k a_k^\dagger a_k + \sigma_+ \sigma_-$ is conserved because $[\hat{N}, H] = 0$. It has been reported in [41] that the total excitation number N in the ground-state of spin-boson model with the RWA form jumps from 0 to 1 at a critical coupling strength. This instability can be also called first-order phase transition, because the first derivative of the ground-state energy is discontinuous. Due to the possible sequence of instabilities with the coupling strength, we can truncate the Hilbert space up to a finite N excitation number. To this end, we first separate the Hilbert space into several subspaces with different excitation numbers $l = 0, 1, 2, \dots, N$. The wave function in l -subspace $|\psi_l\rangle$ can be written explicitly with l excitations. E. g. the wave-functions for $l = 0, 1, 2$ and 3-subspace are listed in the following

$$\begin{aligned} |\psi_0\rangle &= |0\rangle |\downarrow\rangle, \\ |\psi_1\rangle &= c |0\rangle |\uparrow\rangle + \sum_k d_k a_k^\dagger |0\rangle |\downarrow\rangle, \\ |\psi_2\rangle &= \sum_k e_k a_k^\dagger |0\rangle |\uparrow\rangle + \sum_{kk'} f_{kk'} a_k^\dagger a_{k'}^\dagger |0\rangle |\downarrow\rangle, \\ |\psi_3\rangle &= \sum_{kk'} p_{kk'} a_k^\dagger a_{k'}^\dagger |0\rangle |\uparrow\rangle \\ &\quad + \sum_{kk'k''} q_{kk'k''} a_k^\dagger a_{k'}^\dagger a_{k''}^\dagger |0\rangle |\downarrow\rangle. \end{aligned}$$

Then the wavefunction in the truncated Hilbert space up to N excitations can be expressed as

$$|\psi\rangle^{\leq N} = \sum_{l=0}^N |\psi_l\rangle. \quad (6)$$

For $N = 0$, $|\psi\rangle^{\leq 0} = |0\rangle |\downarrow\rangle$, the ground-state energy is $E_0 = -\frac{\Delta}{2}$. However, it is very difficult to obtain the analytical solution for $|\psi\rangle^{\leq N}$ up to $N > 0$ excitations, numerically exact diagonalizations are then required to obtain converged lowest energy. This approach is called NED below.

MCS ansatz.- We also apply the MCS ansatz [28, 29, 33] to the spin-boson model in the RWA. To facilitate the variational study and visualize the symmetry breaking

explicitly, we rotate the Hamiltonian (3) around the y -axis by an angle $\pi/2$, which gives

$$\begin{aligned} H^T &= -\frac{\Delta}{2} \sigma_x + \sum_k \omega_k a_k^\dagger a_k + \frac{1}{2} \sum_k g_k (a_k^\dagger + a_k) \sigma_z \\ &\quad + \frac{\lambda}{2} \sum_k g_k (a_k - a_k^\dagger) i \sigma_y \end{aligned} \quad (7)$$

The trial state $|\psi^T\rangle$ is written in the basis of spin-up state $|\uparrow\rangle$ and spin-down state $|\downarrow\rangle$

$$|\psi^T\rangle = \left(\begin{array}{c} \sum_{n=1}^{N_c} A_n \exp \left[\sum_{k=1}^L f_{n,k} (a_k^\dagger - a_k) \right] |0\rangle \\ \sum_{n=1}^{N_c} B_n \exp \left[\sum_{k=1}^L h_{n,k} (a_k^\dagger - a_k) \right] |0\rangle \end{array} \right), \quad (8)$$

where A_n (B_n) are related to the occupation probabilities of spin-up (spin-down) state in the n th coherent state, N_c and L are numbers of coherent states and total bosonic modes respectively, $f_{n,k}$ ($h_{n,k}$) represents bosonic displacement of the n th coherent state and k th bosonic mode. The symmetric MCS ansatz ($A_n = B_n$ and $f_{n,k} = -g_{n,k}$) can only be applied to the delocalized phase, so one can easily detect the symmetry breaking.

The energy expectation value can be calculated as follows

$$E = \frac{\langle \psi^T | H^T | \psi^T \rangle}{\langle \psi^T | \psi^T \rangle}, \quad (9)$$

where

$$\begin{aligned} \langle \psi^T | H^T | \psi^T \rangle &= \sum_{m,n} (A_m A_n F_{m,n} \alpha_{m,n} \\ &\quad + B_m B_n G_{m,n} \beta_{m,n} - \gamma_{mn} \Gamma_{m,n} A_m B_n), \\ \langle \psi^T | \psi^T \rangle &= \sum_{m,n} (A_m A_n F_{m,n} + B_m B_n G_{m,n}), \end{aligned}$$

with

$$\begin{aligned} F_{m,n} &= \exp \left[-\frac{1}{2} \sum_k (f_{m,k} - f_{n,k})^2 \right], \\ G_{m,n} &= \exp \left[-\frac{1}{2} \sum_k (h_{m,k} - h_{n,k})^2 \right], \\ \Gamma_{m,n} &= \exp \left[-\frac{1}{2} \sum_k (f_{m,k} - h_{n,k})^2 \right], \\ \alpha_{m,n} &= \sum_k \left[\omega_k f_{m,k} f_{n,k} + \frac{gk}{2} (f_{m,k} + f_{n,k}) \right], \\ \beta_{m,n} &= \sum_k \left[\omega_k h_{m,k} h_{n,k} - \frac{gk}{2} (h_{m,k} + h_{n,k}) \right], \\ \gamma_{m,n} &= \left[\Delta + \lambda \sum_k g_k (f_{m,k} - h_{n,k}) \right]. \end{aligned}$$

Minimize energy expectation value with respect to variational parameters gives the following self-consistent

equations

$$\frac{\partial E}{\partial A_n} = \frac{\partial E}{\partial B_n} = \frac{\partial E}{\partial f_{ij}} = \frac{\partial E}{\partial h_{ij}} = 0$$

which leads to

$$\sum_n (2A_n F_{i,n} (\alpha_{i,n} - E) - \Gamma_{i,n} B_n \gamma_{i,n}) = 0, \quad (10)$$

$$\sum_n (2B_n G_{i,n} (\beta_{i,n} - E) - \Gamma_{n,i} A_n \gamma_{n,i}) = 0, \quad (11)$$

$$\sum_n \{-\Gamma_{i,n} B_n (h_{n,j} \gamma_{i,n} + \lambda g_j) + A_n F_{i,n} [2(\alpha_{i,n} + \omega_j - E) f_{n,j} + g_j]\} = 0, \quad (12)$$

$$\sum_n \{-\Gamma_{n,i} A_n (f_{n,j} \gamma_{n,i} - \lambda g_j) + B_n G_{i,n} [2(\beta_{i,n} + \omega_j - E) h_{n,j} - g_j]\} = 0. \quad (13)$$

In practise, these parameters can be obtained by solving the coupled equations self-consistently, which in turn give the ground-state energy and wavefunction. The ground-state with zero excitation $|0\rangle |\downarrow\rangle$ to Hamiltonian (3) can be contained in MCS wavefunction to Hamiltonian (7) by set the constrained coefficients: $A_n = B_n$ and $f_{n,k} = h_{n,k} = 0$ for all n . However the state with nonzero total excitations cannot be included in the MCS ansatz due to the finite number of coherent states. It has been demonstrated that this wavefunction can describe the localized phase of the spin-boson model [31]. The number of the coherent states in the practical calculations in this paper is $N_c = 6$, which is sufficient to judge the existence of the second-order QPT.

For three approaches described above, discretization of the energy spectrum of the continuum bath should be performed at the very beginning in the practical calculations. The same logarithmic discretization is taken for different approaches if comparison is made in the data presented below.

III. RESULTS AND DISCUSSIONS

We will describe our main results by VMPS method to the spin-boson model with the RWA described by Eq. (3) for $\lambda = 1$. Surprisingly, we observe a second-order QPT in spin-boson model under RWA, beyond the widely accepted opinion. In literature, only the full spin-boson model ($\lambda = 0$) for the sub-Ohmic bath undergoes the second-order QPT, while the RWA will induce the first-order QPT. It is further confirmed by the MCS variational approach. The symmetry breaking was unambiguously found above the critical point in this wavefunction based approach. The NED results are also given, which should be exact at the weak coupling, and can be regarded as a benchmark in this regime. Besides the second-order QPT, we also find a few first-order QPTs before the critical point of the second-order QPT for large bath exponent s . As s decreases, the first-order QPTs

disappear successively, but the second-order phase transition remains robust no matter how small s is. We will discuss those phenomena in the following subsections.

A. Magnetization $\langle \sigma_x \rangle$

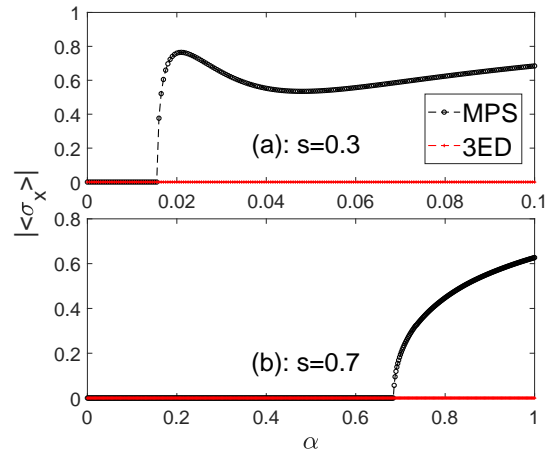


FIG. 1: (Color online) Magnetization $\langle \sigma_x \rangle$ as a function of α in the ground-state for (a) $s = 0.3$ and (b) 0.7 . Black lines with circles denote the VMPS results and the red dashed lines the $N = 3$ -ED ones.

In terms of Hamiltonian (3), magnetization $\langle \sigma_x \rangle$ can be regarded as the order parameter in this model. In the second-order phase transition, due to the symmetry breaking, the order parameter changes from zero to nonzero at the critical points. In Fig. 1 we present the VMPS results for $\langle \sigma_x \rangle$ as a function of the coupling strength α for the spin-boson model in the RWA (i.e. $\lambda = 1$) for two typical values of $s = 0.3$ and 0.7 . The logarithmic discretization parameter $\Lambda = 2$ and $L = 50$ bosonic mods are used for both approaches here, and will be taken below if not specified. Surprisingly, magnetization changes abruptly from zero to nonzero for both cases. The critical points of the second-order QPTs are $\alpha_c = 0.016, 0.685$ for $s = 0.3, 0.7$ respectively.

However, the NED within the excitation number up to N shows that the order parameter $\langle \sigma_x \rangle$ remains zero for all coupling strengths. Note that the VMPS has provided the convincing results for the full spin-model [21]. NED cannot yield the consistent results with the VMPS ones. It is suggested that the total excitation number may not conserve with α due to the unexpected symmetry breaking.

In the finite-size Dicke model with the RWA [42, 43], the system usually undergoes the first-order phase transition, i.e. sequence of instabilities, among the phases within different conserved excitation numbers as the coupling strength increases. In the limit $\Delta/\omega \rightarrow \infty$, the second-order quantum phase transitions have been observed in quantum Rabi model with the RWA [15, 45].

It has been also reported that the Dicke model under the RWA displays a second-order QPT in the thermodynamic limit [11]. Contrary to the Quantum Rabi (Dicke) model in the RWA, the spin-boson model under the RWA could undergo the second-order QPT even for finite value of Δ/ω (one qubit).

B. Effective tunneling matrix $\langle\sigma_z\rangle$ and the ground-state energy

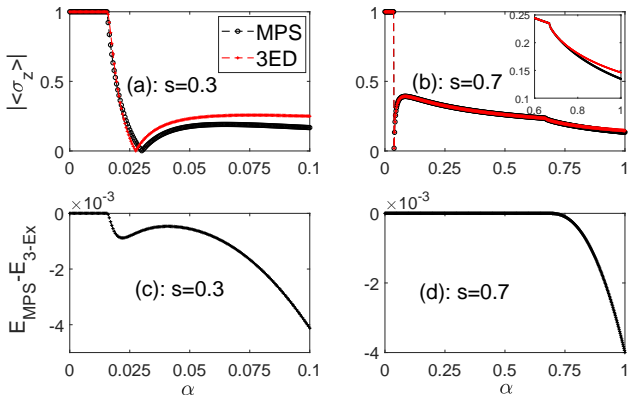


FIG. 2: (Color online) The effective tunneling matrix $\langle\sigma_z\rangle$ (upper panel) and the ground-state energy difference (lower panel) by the VMPS and $N = 3$ ED for $s = 0.3$ (left panel) and 0.7 (right panel).

We then examine the other observables, such as effective tunneling matrix $\langle\sigma_z\rangle$ and the ground-state energy by both VMPS and 3ED, which are exhibited in Fig. 2. Obviously, two observables begin to deviate only after the critical point α_c . Especially we find that for the ground-state energies by the VMPS become lower than those by 3ED after the critical points, indicating again the invalidity of ED method at the strong coupling. Practically, we cannot perform ED with the very large total excitation number due to the huge Hilbert space. In this paper, our exact diagonalization is only performed up to $N = 3$. Of course, if one can really perform the true exact diagonalization without the limitation of the total excitation numbers, the true ground-state could be correctly described.

C. The parity symmetry breaking

It is well known that the spin-boson model with (without) the RWA possesses a $U(1)$ (Z_2) symmetry, which is characterized by the action of the operator

$$\mathfrak{R}(\theta) = \exp(i\theta\hat{N}),$$

where the arbitrary angle θ corresponds to $U(1)$ symmetry and the special value of $\theta = \pi$ to Z_2 symmetry. $U(1)$

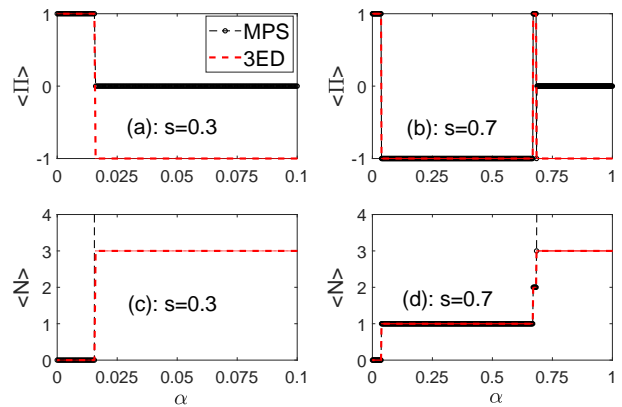


FIG. 3: (Color online) Parity (upper panel) and total excitations (lower panel) in the ground-state by the three-excitation NED and the present VMPS for $s = 0.3$ and 0.7

is a higher symmetry than Z_2 , so in the RWA spin-boson model, the system also has Z_2 symmetry, i.e. the parity symmetry, like that in the full spin-boson model. For the conserved parity, there are two eigenvalues: ± 1 . In this section, we study the behaviour of the expectation value of the parity $\hat{\Pi} = \exp(i\pi\hat{N})$.

The finite order parameter above the critical points obtained by VMPS in the previous subsection displays the spontaneous symmetry breaking, while parity is generally just the criterion to determine whether symmetry is broken. The upper panel in Fig. 3 gives the expectation value of parity $\langle\hat{\Pi}\rangle$ obtained by both methods for $s = 0.3, 0.7$. Before the critical points, both methods yield the same results for the parity. It is interesting to find that in this regime, the value of parity for all values of $s < 1$ is either 1 or -1 , which corresponds to even or odd parity respectively. It follows that the symmetry is not broken in this regime. Nevertheless, the average parity $\langle\hat{\Pi}\rangle$ becomes zero above the critical points. It is not the eigenstate of the parity operator, indicating the spontaneous parity symmetry breaking. We have also observed the similar behavior for the parity in the sub-Ohmic spin-boson model without the RWA (not shown here).

To detect the possible first-order phase transitions, we also present the average value of the total excitation number $\langle\hat{N}\rangle$ as a function of the coupling strength in the lower panel of Fig. 3. Below the critical points, it is shown that $\langle\hat{N}\rangle$ by both approaches jumps between different plateaus with different integers, demonstrating first-order phase transitions, like in the JC model [15]. Above the critical points, $\langle\hat{N}\rangle$ by VMPS increases abruptly, indicating that N is not conserved in this regime. The NED approach can only describe the phase with excitation number less than or equal to N . The total excitation

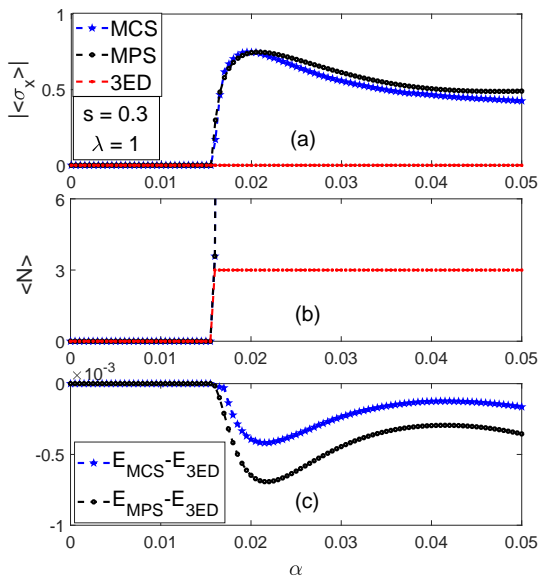


FIG. 4: (Color online) (a) The order parameter $\langle \sigma_x \rangle$, (b) the total excitations $\langle N \rangle$ as a function of the coupling strength within VMPS, 3ED, and MCS variational approaches. (c) The difference between the VMPS (MCS) ground-state energy and that by 3ED. $s = 0.3$.

number is not limited in VMPS, so it can describe all phases very well. For $s = 0.7$, the total excitation number N by both approaches increases from 0 to 2 before α_c , demonstrating first-order phase transitions successively.

Therefore, we find the rich phase transitions in the sub-Ohmic spin-boson model with the RWA. First, the second-order QPT occurs for any finite model parameters, similar to its counterpart without the RWA. In both Rabi model and Dicke model with the RWA, the second-order QPTs cannot happen for finite ratio Δ/ω or finite qubit number. Second, for larger bath exponents, e.g. $s = 0.7$, both the first- and second-order QPTs occur subsequently with the coupling strength. Several first-order phase transitions before the critical points indicate sequence of instabilities. The first-order phase transition is absent for small bath exponent s , such as for $s = 0.3$.

D. Evidence for the second-order QPT by MCS variational studies

Since this model at $s = 0.3$ exhibits only one second-order QPT from the zero excitation ground-state, we can employ the MCS variational approach to provide additional evidence, because both the states with zero excitation and in the localized phase can be described by this wavefunction ansatz. In Fig. 4, we list results by both MCS, VMPS, and $N = 3$ ED approaches for $s = 0.3$. The logarithmic discretization parameter $\Lambda = 2$ and $L = 20$ bosonic modes are taken for all three approaches here.

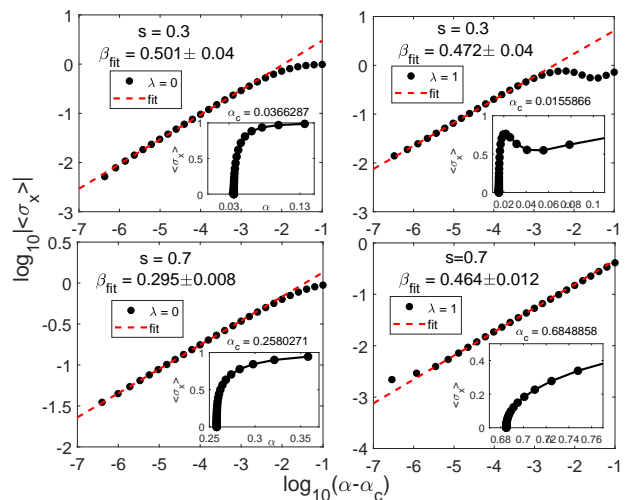


FIG. 5: (Color online) The log-log plot of the magnetization as a function of $\alpha - \alpha_c$ of the spin-boson model with (right) and without (left) the RWA for $s = 0.3$ (upper panel) and $s = 0.7$ (lower panel). The numerical results by VMPS are denoted by black circles, and the power law fitting curves by the red dashed lines. All insets show the corresponding linear plots.

Note that the number of bosonic modes here are smaller than those in other figures due to the computational difficulties in the MCS approach, but it does not influence the essential results at all. The MCS approach is used here to account for the existence of the second-order QPT qualitatively, not for the precise location of the critical points.

Before the critical points, the results by all three methods are the same. Nonzero order parameter $|\langle \sigma_x \rangle|$ by MCS approach appear above the critical points, providing a further convincing evidence of the spontaneous symmetry breaking. The MCS ground state energies are lower than those by NED method after the critical point, indicating that the state with broken symmetry is more stable. The total excitation number by MCS method increases suddenly above the critical point, because of no limitation of total excitation number in coherent state. All these findings in the MCS variational study provide strong evidence of the second-order QPT in spin-boson model with RWA. As found recently by Blunden-Codd et al. [31] that the very accurate wave function can be only obtained by at least a hundred of single-mode coherent states, so by $N_b = 6$ coherent states, the MCS results for the order parameter and energy still slightly deviate from those by VMPS above the critical points.

E. The critical exponent for magnetization

Now we will study the nature of the second-order QPT in the sub-Ohmic spin-boson model under RWA. The na-

ture question is whether the RWA changes the universality of the second-order QPT. Note that the most important critical exponent in the second-order QPT is the order parameter one β , which can be determined through the displayed power-law behavior near the critical point $\langle \sigma_x \rangle \propto (\alpha - \alpha_c)^\beta$. Previously, the order-parameter exponent in the full spin-boson model has been calculated with different advanced approaches [18–21, 25]. It is now generally accepted that the order-parameter exponent takes the mean-field value $\beta = 0.5$ for $s < 1/2$, and non-classical one $\beta < 0.5$ for $s > 1/2$.

We present the magnetization by the VMPS method as a function of $\alpha - \alpha_c$ in a log-log plot for both $\lambda = 1$ (RWA) and $\lambda = 0$ (non-RWA) in Fig. 5. A very nice power-law behavior over three decades is demonstrated in all cases. The results for the full model are nearly the same as those in the Ref. [21]. One can find that β is around 0.5 for $s < 1/2$ for both cases. Very surprisingly, even for $s = 0.7$ in the RWA model, we still obtain $\beta = 0.464$ within the statistical error, indicating that the RWA results still exhibit the mean-field critical behaviour ($\beta \approx 0.5$) for $s > 1/2$, in sharp contrast to the full model without the RWA [21]. In the QPT of the quantum Rabi model with different anisotropic constants in the limit $\Delta/\omega \rightarrow \infty$ [15, 44–46], the critical exponent α_{sg} of the spectral gap near the critical point depends crucially on the counter-rotating terms. $\alpha_{sg} = 1$ for the JC model [15], and it jumps to $\alpha_{sg} = 0.5$ if any counter-rotating coupling terms set in [44–46]. So the counter-rotating coupling terms may play important role on the critical exponents in the QPT.

F. Extensions to the Ohmic bath.

Now we turn to the Ohmic spin-boson model under the RWA. By both VMPS and the 3ED methods, the above observables are also calculated. In Fig. 6, we collect magnetization $\langle \sigma_z \rangle$, parity $\langle \hat{\Pi} \rangle$, and the total excitations $\langle N \rangle$ as a function of the coupling strength α in the range (0, 2). During this wide regime, one can find the model undergoes a few first-order QPT with the increment 1 of the total excitation number. The two approaches almost give the same results. It follows that in the Ohmic bath, the 3ED approach is suited to the wide coupling regime where no second-order QPT occurs. Actually we have also studied the super-Ohmic bath $s = 3/2$, and find that there is only one first-order QPT in the regime $\alpha = [0, 2]$ (not shown here).

IV. CONCLUSION

In this work, we study the spin-boson model in the RWA by the VMPS method, MCS variational ansatz, and exact diagonalizations within the truncated Hilbert

space. Surprisingly, we find the second-order QPT in the

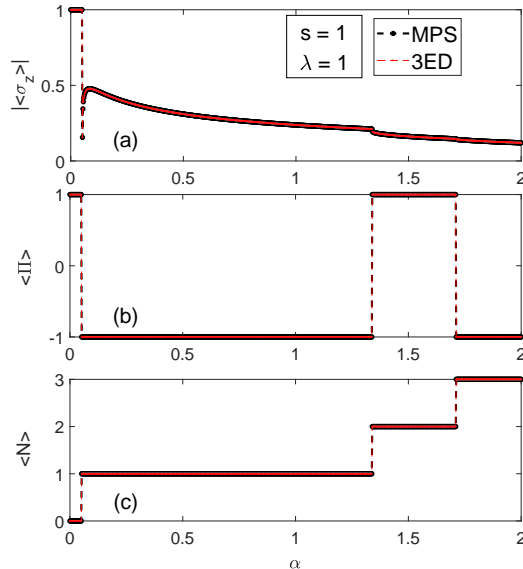


FIG. 6: (Color online) (a) The order parameter $\langle \sigma_x \rangle$, (b) parity $\langle \hat{\Pi} \rangle$, and (c) the total excitations $\langle N \rangle$ as a function of the coupling strength within VMPS and 3ED approaches for the Ohmic bath.

RWA model for any bath exponent $s < 1$ for the first time, to the best of our knowledge. A rich picture for the quantum phase transitions is observed. Besides the second-order phase transition, the first-order phase transition also appears in the same model, which could only vanish for small bath exponents. This phenomenon has been never observed in the other spin-boson like model, such as the quantum Rabi and Dicke models in the RWA. Note that the second-order QPT could exist in the latter models only in thermodynamic limits, such as ratio $\frac{\Delta}{\omega} \rightarrow \infty$ or the atomic number $N \rightarrow \infty$, which is not required here.

Within the statistical error, the mean-field exponent is observed for all values of the bath exponents $s < 1$, in contrast to the full spin-boson model with the counter rotating terms. It is then suggested that the counter-rotating wave terms would change the order parameter exponent for $1/2 < s < 1$. The analytical argument about the quantum-to-classical mapping [47–49] in the spin-boson model in the RWA will be helpful to account for the robust mean-field nature observed here for all sub-Ohmic bath exponent $0 < s < 1$.

ACKNOWLEDGEMENTS This work is supported by the National Science Foundation of China (Nos. 11474256, 11834005), the National Key Research and Development Program of China (No. 2017YFA0303002).

* Email:qhchen@zju.edu.cn

-
- [1] A. J. Leggett et al., Rev. Mod. Phys. **59**, 1(1987).
- [2] M. O. Scully and M. S. Zubairy, *Quantum Optics* (Cambridge University Press, Cambridge, 1997).
- [3] H. P. Breuer and F. Petruccione, *The Theory of Open Quantum Systems* (Oxford University Press, New York, 2002).
- [4] U. Weiss, *Quantum Dissipative Systems* (World Scientific Publishing Company, 2008).
- [5] T. Niemczyk et al., Nature Physics **6**, 772 (2010).
- [6] F. Yoshihara, T. Fuse, S. Ashhab, K. Kakuyanagi, S. Saito, and K. Semba, Nat. Phys. **13**, 44 (2016).
- [7] F. Dimer, B. Estienne, A. S. Parkins, and H. J. Carmichael, Phys. Rev. A **75**, 013804 (2007); K. Baumann, C. Guerlin, F. Brennecke, and T. Esslinger, Nature (London) **464**, 1301 (2010).
- [8] J. I. Cirac, A. S. Parkins, R. Blatt, and P. Zoller, Phys. Rev. Lett. **70**, 556 (1993).
- [9] P. Forn-Díaz, J. J. García-Ripoll, B. Peropadre, J.-L. Orgiazzi, M. A. Yurtalan, R. Belyansky, C. M. Wilson, and A. Lupascu, Nat. Phys. **13**, 39 (2016).
- [10] J. Keeling, M. J. Bhaseen, and B. D. Simons, Phys. Rev. Lett. **105**, 043001 (2010).
- [11] A. Baksic and C. Ciuti, Phys. Rev. Lett. **112**, 173601 (2014).
- [12] Q. T. Xie, S. Cui, J. P. Cao, L. Amico, and H. Fan, Phys. Rev. X **4**, 021046 (2014).
- [13] A. L. Grimsmo and S. Parkins, Phys. Rev. A **87** 033814 (2013).
- [14] M. Tavis and F. Cummings, Phys. Rev. **170**, 379 (1968).
- [15] M.-J. Hwang and M. B. Plenio, Phys. Rev. Lett. **117**, 123602 (2016).
- [16] E. T. Jaynes and F.W. Cummings, Proc. IEEE **51**, 89(1963).
- [17] R. Bulla, N. Tong, and M. Vojta, Phys. Rev. Lett. **91**, 170601 (2003); M. Vojta, N. Tong, and R. Bulla, Phys. Rev. Lett. **94**, 070604 (2005); R. Bulla, Phys. Rev. Lett. **102**, 249904(E) (2009); M. Vojta, N. H. Tong, and ev. B **81**, 075122 (2010); N. H. Tong and Y. H. Hou, Phys. Rev. B **85**, 144425(2012).
- [18] A. Winter, H. Rieger, M. Vojta, and R. Bulla, Phys. Rev. Lett. **102**, 030601 (2009).
- [19] A. Alvermann and H. Fehske, Phys. Rev. Lett. **102**, 150601 (2009).
- [20] Y.-Y. Zhang, Q.-H. Chen, and K.-L. Wang, Phys. Rev. B **81**, 121105(R)(2010).
- [21] C. Guo, A. Weichselbaum, J. von Delft, and M. Vojta, Phys. Rev. Lett. **108**, 160401 (2012).
- [22] M. F. Frenzel and M. B. Plenio, New Journal of Physics **15**, 073046(2013).
- [23] R. Silbey, and R. A. Harris, J. Chem. Phys. **80**, 2615 (1984).
- [24] Z. G. Lu and H. Zheng, Phys. Rev. B. **75**, 054302(2007).
- [25] A. W. Chin, J. Prior, S. F. Huelga and M. B. Plenio, Phys. Rev. Lett. **107**, 160601 (2011).
- [26] C. K. Lee, J. M. Moix, and J. Cao, J. Chem. Phys. **136**, 204120 (2012); C. K. Lee, J. Cao, and J. B. Gong Phys. Rev. E **86**, 021109 (2012).
- [27] H. Zheng and Z. G. Lu, J. Chem. Phys. **138**, 174117 (2013).
- [28] S. Bera, S. Florens, H. U. Baranger, N. Roch, A. Nazir, A. W. Chin, Phys. Rev. B **89**, 121108(R) (2014); S. Bera, A. Nazir, A. W. Chin, H. U. Baranger, S. Florens, Phys. Rev. B **90**, 075110 (2014).
- [29] L. Duan, S. He, Q.-H. Chen, arXiv:1412.6343.
- [30] N. Zhou, L. Chen, Y. Zhao, D. Mozyrsky, V. Chernyak, Y. Zhao, Phys. Rev. B **90**, 155135(2014).
- [31] Z. Blunden-Codd, S. Bera, B. Bruognolo, N.-O. Linden, A. W. Chin, J. von Delft, A. Nazir, and S. Florens, Phys. Rev. B **95**, 085104 (2017).
- [32] S. He, Li. W. Duan, and Q. -H. Chen, Phys. Rev. B **97**, 115157 (2018)
- [33] Q. B. Ren, Q. H. Chen, Chin. Phys. Lett. **22**, 2914 (2005).
- [34] U. Schollwöck, Annals of Physics **326**, 96(2011).
- [35] V. Zauner-Stauber, L. Vanderstraeten, M. T. Fishman, F. Verstraete, and J. Haegeman, Phys. Rev. B **97**, 045145 (2018).
- [36] A. W. Chin, A. Rivas, S. F. Huelga, and M. B. Plenio, Journal of Mathematical Physics **51**, 092109 (2010).
- [37] F. A. Y. N. Schröder, A. W. Chin, Phys. Rev. B **93**, 075105 (2016).
- [38] A. Weichselbaum, F. Verstraete, U. Schollwöck, J. I. Cirac, and J. von Delft, Phys. Rev. B **80**, 165117 (2009).
- [39] H. Saberi, A. Weichselbaum, and J. von Delft, Phys. Rev. B **78**, 035124 (2008).
- [40] U. Schollwöck, Ann. Phys. (Leipzig) **326**, 96 (2011).
- [41] Q.-J. Tong, J.-H. An, H.-G. Luo, and C. Oh, Phys. Rev. B **84**, 174301 (2011).
- [42] Y.-Y. Zhang, T. Liu, K.-L. Wang, and Q.-H. Chen, Optics Communications **283**, 3459(2010)
- [43] V. Bužek, M. Orszag, M. Roško, Phys. Rev. Lett. **94**, 163601 (2005).
- [44] M.-J. Hwang, R. Puebla, and M. B. Plenio, Phys. Rev. Lett. **115**, 180404 (2015).
- [45] M. Liu, S. Chesi, Z.-J. Ying, X. Chen, H.-G. Luo, and H.-Q. Lin, Phys. Rev. Lett. **119**, 220601 (2017).
- [46] L.-T. Shen, Z.-B. Yang, H.-Z. Wu, and S.-B. Zheng Phys. Rev. A **95**, 013819 (2017).
- [47] M. Vojta, Phys. Rev. B **85**, 115113 (2012)
- [48] S. Kirchner, J. Low Temp. Phys. **161**, 282 (2010).
- [49] S. Kirchner, Q. Si, and K. Ingersent, Phys. Rev. Lett. **102**, 166405 (2009); S. Kirchner, K. Ingersent, and Q. Si, Phys. Rev. B. **85**, 075113(2012).